PHYSICAL REVIEW D **93,** 083504 (2016)

Leptophilic dark matter in Galactic Center excess

Bo-Qiang Lu[1,2] and Hong-Shi Zong[1]

[1]*School of Physics, Nanjing University, Nanjing 210093, China*

[2]*Key Laboratory of Dark Matter and Space Astronomy, Purple Mountain Observatory, Chinese Academy of Sciences, Nanjing 210008, China*

(Received 4 November 2015; published 6 April 2016; corrected 22 April 2016)

Herein we explore the possibility of explaining a gamma-ray excess in the Galactic Center with the dark matter scenario. After taking into account the constraints from both the AMS-02 experiment and the gamma-ray observation on dwarf spheroidal satellite galaxies in Fermi-LAT, we find that the τ lepton channel is the only permissive channel for the interpretation of the Galaxy center excess. Tau leptophilic dark matter provides a well-motivated framework in which the dark matter can dominantly couple to τ lepton at tree-level. We describe the interactions with a general effective field theory approach by using higher-dimensional operators, and this approach provides for a model independent analysis. We consider the constraints from the measurement of the DM relic density in the Planck experiment and the AMS-02 cosmic rays experiment, and find that most of the interaction operators except $\mathcal{O}_7$, $\mathcal{O}_9$ and $\mathcal{O}_{12}$ have been excluded. Due to the quantum fluctuations, even in such a scenario there are loop induced dark matter-nucleon interactions. We calculate the dark matter-nucleon scattering cross-section at loop-level, and if the limits on the dark matter-nucleon scattering cross-section from direct detection experiments are also taken into account, we find that the operators remaining available for accounting for the Galaxy center excess are $\mathcal{O}_9$ and $\mathcal{O}_{12}$.

DOI: 10.1103/PhysRevD.93.083504

I. INTRODUCTION

Although cosmological and astrophysical observations have shown that the majority of the matter in the Universe consists of cold dark matter (DM) rather than standard model (SM) particles [1,2], the nature of dark matter (DM) still remains mysterious. The most appealing DM particle candidates are the so-called weakly interacting massive particles (WIMPs), and it is also widely believed that WIMPs could annihilate one another and then generate (or alternatively decay into) stable particles, such as high energy γ—rays and pairs of lepton and quark [1,3,4]. In the hypothesis of a flat ΛCDM cosmology, the large-scale simulations of galaxy formation predict extensive, centrally concentrated, dark matter halos around galaxies. Since the self-annihilation probability of DM is proportional to the DM density, this implies that the indirect DM signal should be enhanced in the Galactic Center (GC). Using observation gamma ray data from the Fermi-LAT satellite, and after a careful subtraction of the diffuse emissions from known astrophysical sources, several independent groups have found an extended excess in the gamma ray at the GC and the peak is appears to be at energies around (1–3) GeV [5–9]. A recent analysis of GC gamma ray data by the Fermi-LAT Collaboration also shows an excess in the GC after subtracting the interstellar emission and point-source contributions [10]. While this excess could be attributed to astrophysical sources, such as the central point sources or unresolved millisecond pulsars [11–14], in the following, we focus on the DM interpretations of the Fermi GeV excess and, therefore, no further discussion of potential astrophysical explanations is given. It has been shown that its spectrum and morphology are compatible with the gamma rays produced in the annihilation of DM to leptons or quarks [7,15–18]. As many works have yielded similar constraints on the DM parameter space [17–21] by using the Fermi–LAT data, herein we make use only of the most recent results from Ref. [18]. In this work, we adopt an effective interaction approach to describe the interactions of the DM particles with the SM particles by using higher-dimensional operators, and this method does not commit to any particular DM model and thus is a model independent analysis. Recently, a number of works have used this approach to deal with different observable signals in various experiments [22–29]. This approach simply assumes that the DM particle exists in a hidden sector, which communicates to the SM sector via a heavy mediator. This heavy mediator can be integrated out at an energy scale well below the interaction energy scale, and thus the interactions can be conveniently described by a set of effective interactions. The strength of each interaction depends on the nature of the DM particle and the mediator [22,24,25]. Using the effective field interaction and with the assumption that DM only couples to quark families, in work [29], they find that only a very small set of operators can explain the Galactic Center excess (GCE) while being consistent with other constraints such as direct detection as well as Large Hadron Collider (LHC) research. Using AMS-02 antiproton ratio and positron fraction data, we derive stringent limits on the dark matter annihilation

cross-section and lifetime at 95% C.L. [30]. Further we find that the quark channels have been excluded by the AMS-02 data, while the τ lepton channel is still allowed (as shown in Fig. 1 and following discussion). Motivated by this conclusion, in this work we assume that the DM sector has no direct couplings to quarks, but only to leptons at tree-level, and in particular the τ lepton. We are aware that our hypothesis is similar to the leptophilic DM scenario, in which DM recoils against electrons bound in atoms, and that it has been proposed as an explanation for the annually modulated scintillation signal in DAMA/LIBRA versus the absence of a signal for nuclear recoils in experiments like CDMS or XENON10 [24]. But we emphasize that in our scenario DM does not couple to electron or μ lepton directly but only to τ lepton with the AMS-02 data under-consideration (see the following discussions for details), while the leptophilic DM scenario assumes a tree-level coupling to the electron. However, due to the quantum fluctuations, even in such a scenario there are loop induced DM-nucleon interactions, where photons emitted from virtual leptons couple to the charge nucleus [24]. Noting these, the constraints from direct detection of the interactions of DM-lepton are also taken into account. Furthermore, we also consider the constraints from the measurement of the cosmic microwave background anisotropies in the Planck experiment and the AMS-02 cosmic rays experiment. Though demanding an operator that satisfies the current experimental constrains from direct and indirect detection and does not give too much relic density to the Universe, we rule out most of the effective interaction operators.

This work is arranged as follows. In Sec. II we briefly introduce the effective interactions considered in this work. In Sec. III, we introduce the τ leptophilic dark matter model and show that such a model is required by constraints from various DM detection experiments. In Sec. IV, we put limits on the effective field theory by taking into account constraints from DM relic density observation, direct and indirect. We summarize our results in Sec. V.

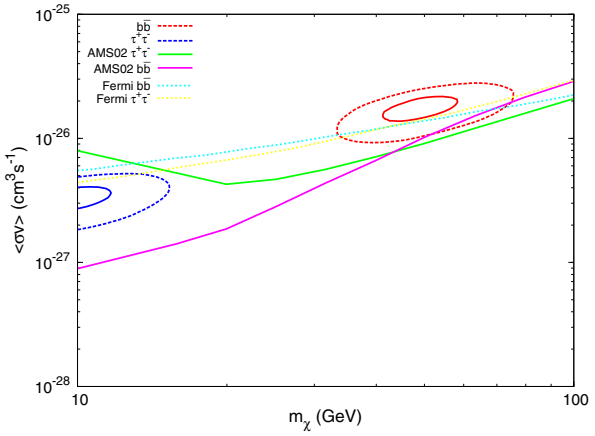

FIG. 1. DM annihilation cross section as a function of DM mass m_χ, the solid (dot) cycle corresponding to 1σ (3σ) contours from [18], the solid green and pink line is the upper limits of DM annihilation cross section at 95% C.L. from [30], the dot light blue and yellow line is the upper limits of DM annihilation cross section at 95% C.L. from [48].

II. THE EFFECTIVE FIELD INTERACTION

We use the effective field operators to describe the interactions between WIMPs particles and SM particles (in the following, we will assume that the DM particle is a Dirac fermion or a complex scalar, use χ to stand for it. And f stands for a SM fermion). This approach is based on the following assumptions: (i) the WIMP is a singlet under the SM gauge groups, thus possesses no couplings to the electroweak gauge bosons at tree-level, (ii) the WIMPs may interact with the SM particles through a dark gauge sector, this symmetry is spontaneous breaking at low energy and leading to a suppression of the interaction between WIMPs and SM particles. The mass scale of particles conducting the interaction between WIMPs and the SM particles are much larger than typical reaction energy, and therefore can be integrated out from the Lagrangian. Operators higher than dimension 7 are not taken into account since they are highly suppressed by the mass scale. In addition to these requirements, we also require that the interact currents fulfill Z_2 symmetry both for DM and SM sectors. The effective interactions considered in this work are shown in Table I. Among these operators, the DM particle included in the interactions ($\mathcal{O}_1$–$\mathcal{O}_{10}$) is a Dirac fermion, while in the interactions ($\mathcal{O}_{11}$–$\mathcal{O}_{14}$) the DM particle is a complex scalar. The interaction types include (axial-) vector type exchange ($\mathcal{O}_1$–$\mathcal{O}_4$), tensor type exchange ($\mathcal{O}_5$–$\mathcal{O}_6$), or (pseudo-) scalar type exchange ($\mathcal{O}_7$–$\mathcal{O}_{10}$). The SM particle mass m_f dependence on the coupling strength that comes from DM models with scalar exchange diagrams [25]. Depending on the Lorentz structure of the operator, dark matter annihilation processes can be unsuppressed, chirality suppressed, p-wave suppressed, or suppressed by both of the above [29,31]. Chirality suppression depends on the mass of the SM fermion involved in the process, which means that sufficiently heavy DM is much more weakly suppressed to annihilate into heavy SM particles than to annihilate into light SM particles, thus for chirality suppressed operators, DM particles primarily annihilate into top quarks or τ leptons. On the other hand, the p-wave suppression is connected to the low velocity of annihilating WIMPs [31]. For example, the tensor-type interaction $\mathcal{O}_5$ and pseudoscalar type interaction $\mathcal{O}_{10}$ are chirality suppressed; axial-vector type interaction $\mathcal{O}_6$ is p-wave suppressed, and the scalar-type interaction $\mathcal{O}_9$ is suppressed by both. With these features, one can expect that DM signals are more likely to be probed in the indirect detections than at colliders for those operators which are suppressed by SM chirality, while those operators which are p-wave suppressed are more easily probed at colliders than in the

indirect detections. The collider could put strong limits on the effective interactions in which the DM currents are contacted with quarks, however it becomes inadequate when the final states are leptons. On the other hand, the indirect detection does not suffer this limitation, and it can give strong limits not only on the quark final states but also on the lepton final states [30]. And for the case of direct detections, DM particles may interact with the nucleons in a detector at a very low relative velocity. As shown in Ref. [25], in the nonrelativistic limit one can find that the spatial components of vector DM current $\bar{\chi}\gamma_\mu\chi$ are not suppressed by v/c, while the spatial components of axial-vector DM current $\bar{\chi}\gamma_\mu\gamma_5\chi$ are suppressed by v/c. In this work, in the nonrelativistic limit only six operators are relevant for the direct detections, namely $\mathcal{O}_1$, $\mathcal{O}_4$, $\mathcal{O}_5$, $\mathcal{O}_7$, $\mathcal{O}_{11}$, and $\mathcal{O}_{13}$. We summarize some of the features of the operators discussed in this section in Table I.

The advantages of the model-independent Effective field theory (EFT) method are obvious; the greatest power of the method is that it is very generic. One can write down the possible operators describing DM interaction and place bounds on each of them from the null results of colliders, direct detection, and/or indirect searches. However, we should bear in mind that this method breaks down when the typical reaction energy is much higher than the mediator mass, and this method also suffers from its ultraviolet completion (UV) incompleteness. Recently, the simplified models have been proposed which go beyond the EFT method [12,32–38]. In the simplified model there is no need to worry about restricting the integration over phase space and it avoids the breakdown of the EFT associated with perturbative unitarity of the contact interactions [36]. It can be understood as a phenomenological sketch of a complete model; for instance, in the minimal supersymmetric standard model this might include only looking at the two lightest supersymmetric particles [35].

TABLE I. List of operators that we use in this work. The forth column indicates whether the primary direct detection signal due to that operator is spin independent (SI), spin dependent (SD), or strongly suppressed (N/A).

Name	Operator	NR limit (Direct Detection)	SI/SD	D/C (Dirac or Complex)
$\mathcal{O}_1$	$\frac{1}{\Lambda_1^2}\bar{\chi}\gamma_\mu\chi\bar{f}\gamma^\mu f$	Yes	SI	D
$\mathcal{O}_2$	$\frac{1}{\Lambda_2^2}\bar{\chi}\gamma_\mu\gamma_5\chi\bar{f}\gamma^\mu f$	No	N/R	D
$\mathcal{O}_3$	$\frac{1}{\Lambda_3^2}\bar{\chi}\gamma_\mu\chi\bar{f}\gamma^\mu\gamma_5 f$	No	N/R	D
$\mathcal{O}_4$	$\frac{1}{\Lambda_4^2}\bar{\chi}\gamma_\mu\gamma_5\chi\bar{f}\gamma^\mu\gamma_5 f$	Yes	SD	D
$\mathcal{O}_5$	$\frac{1}{\Lambda_5^2}\bar{\chi}\sigma_{\mu\nu}\chi\bar{f}\sigma^{\mu\nu} f$	Yes	SD	D
$\mathcal{O}_6$	$\frac{1}{\Lambda_6^2}\bar{\chi}\sigma_{\mu\nu}\gamma_5\chi\bar{f}\sigma^{\mu\nu} f$	No	N/R	D
$\mathcal{O}_7$	$\frac{m_f}{\Lambda_7^3}\bar{\chi}\chi\bar{f}f$	Yes	SI	D
$\mathcal{O}_8$	$\frac{m_f}{\Lambda_8^3}\bar{\chi}\gamma_5\chi\bar{f}f$	No	N/R	D
$\mathcal{O}_9$	$\frac{m_f}{\Lambda_9^3}\bar{\chi}\chi\bar{f}\gamma_5 f$	No	N/R	D
$\mathcal{O}_{10}$	$\frac{m_f}{\Lambda_{10}^3}\bar{\chi}\gamma_5\chi\bar{f}\gamma_5 f$	No	N/R	D
$\mathcal{O}_{11}$	$\frac{m_f}{\Lambda_{11}^2}\chi^\dagger\overleftrightarrow{\partial}_\mu\chi\bar{f}\gamma^\mu f$	Yes	SI	C
$\mathcal{O}_{12}$	$\frac{m_f}{\Lambda_{12}^2}\chi^\dagger\overleftrightarrow{\partial}_\mu\chi\bar{f}\gamma^\mu\gamma_5 f$	No	N/R	C
$\mathcal{O}_{13}$	$\frac{m_f}{\Lambda_{13}^2}\chi^\dagger\chi\bar{f}f$	Yes	SI	C
$\mathcal{O}_{14}$	$\frac{m_f}{\Lambda_{14}^2}\chi^\dagger\chi\bar{f}\gamma_5 f$	No	N/R	C

III. τ LEPTOPHILIC DARK MATTER

For the DM interpretation of the GCE, one should simultaneously take into account constraints from direct experiments, indirect detection and collider research. With the first AMS-02 result (i.e., the positron fraction up to ~350 GeV [39]), assuming that the positron fraction excess is mainly due to astrophysical processes and uses the same phenomenological parametrization as the AMS collaboration in their analysis [39], Bergström *et al.*, [40] obtained very stringent limits on dark matter annihilating or decaying to leptonic final states. Later, the positron flux data or alternatively the electron flux data has been adopted to set limits on the dark matter annihilation/decay channels [41,42]. Recently, the AMS-02 antiproton-to-proton ratio data has been announced in a dedicated conference [43] and the high energy part seems to be in excess of the regular prediction from the conventional cosmic ray propagation model. However, as pointed out by Blasi *et al.* [44–47] that the secondary CRs (positron and antiproton) can also be produced and accelerated in the SNR source. In this scenario, the "excesses" in positron and antiproton are due to the secondary products of hadronic interactions inside the SNRs. The dense environment and old SNRs are the most important ingredients for the production of positron and antiproton. And the crucial physical process which leads to a natural explanation of the positron and antiproton flux are the fact that the secondary production takes place in the same region where primary CRs are being accelerated [45]. In such a scenario, one can naturally explain the AMS-02 positron fraction and antiproton ratio simultaneously while a new class of source such as DM or pulsars is not required. Following the phenomenological AMS parametrization approach, in Ref. [30] we parametrize the contribution of the SNR with a simple function and place limits on the DM parameters. We find that our results are similar to (or a little stronger than) the limits given by Ackermann *et al.*, [48] which derived from the Fermi-LAT gamma-ray Pass 8 data observation on the dwarf spheroidal satellite galaxies (see Fig. 1 and [30]).

Recently, assuming that the GCE contributes from DM annihilation, Calore *et al.*, [18] gave the 3σ C.L. DM parameter room for various DM annihilation channels. For the quark channels the fit results of DM mass are in the range of (24–50) GeV, and the annihilation cross-sections are in the range of $(1\text{–}3)\times 10^{-26}$ cm^{-3} s^{-1} [18]. These

results are very close to the ideal WIMPs, however, as shown in Fig. 1, we find that such DM parameter spaces have been excluded by AMS-02 data [30], and the constraints derived from the observation on the dwarf spheroidal satellite galaxies in Fermi-LAT [48] also confirmed this conclusion. For the lepton channels, one should also take into account the role of inverse Compton scattering (ICS) emission at higher latitudes [10,18,49]. The DM model that has a mainly branching ratio to monochromatic e^+e^- is severely constrained by the positron fraction data from the AMS-02 experiment [40]. And as pointed out by Calore *et al.*, [18], for any DM mass the annihilation channel to monochromatic e^+e^- would lead to an ICS gamma-ray spectrum with a hard cutoff at the mass threshold, which is in tension with the fact that the Fermi GeV excess spectrum has a very broad peak at $\simeq$2 GeV, making such a model an improbable one in the context of the Fermi GeV excess. And they also find a poor fit result for $\mu^+\mu^-$ channel without accounting for Inverse Compton Scattering emission. The fit becomes good after taking the ICS emission into account, and the DM mass is between (60–70) GeV, and the annihilation cross-section is in the range of $(2\text{–}12)\times 10^{-26}$ cm^{-3} s^{-1}. However, this result also has been excluded by the AMS-02 experiment [30,40,42]. Thus, one finds that the $\tau^+\tau^-$ lepton is the only channel which is allowed given constrains from both the AMS-02 experiment and the gamma-ray observation on dwarf spheroidal satellite galaxies in Fermi-LAT. ICS emission is not important for DM annihilation into $\tau^+\tau^-$, the reason is that while a significant portion of the annihilation power does go into e^+e^- after DM annihilation into $\tau^+\tau^-$, the prompt gamma-ray emission (which produces through the annihilation or decay of $\tau^+\tau^-$) has a very prominent spectral bump, that cannot be smoothed out significantly by including the ICS contribution [18].

In this work we only pay attention to the operators in which the SM factors are fermion bilinear. Specifically, constrains on quark bilinear operators are widely studied in Large Hadron Collider (LHC) searches and other direct detection. And as shown above, the DM interpretation of the GCE with quark channels has been excluded in a model-independent way. Thus, we come to the leptophilic DM scenario, in which the SM factors in the operators are lepton bilinear and the DM sector has no direct couplings to quarks. In such a scenario, the WIMPs interact with the atoms in a detector mainly through the electrons bound in the atoms, there are three types of signals of the interactions [24,50]: (i) the whole recoil is absorbed by the electron that is then kicked out of the atom to which it was bound, (ii) the electron on which the WIMPs scatters remains bound and the recoil is taken up by the whole atom, (iii) interactions between WIMPs and nucleons are induced at loop level. This scenario could account for the DAMA annual modulation signal, but is in conflict with the direct detection experiments such as XENON and CDMS. We have emphasized that different from the leptophilic DM scenario, in our hypothesis WIMPs do not couple to the electron or μ lepton directly, but only to the τ lepton. Thus in our scenario, only the interaction between WIMPs and nucleons induced at loop level takes place in a detector.

IV. CONSTRAINTS ON THE EFFECTIVE INTERACTION

A. Cosmic rays sources and indirect detection

The strategy of indirect detection makes use of the scenario that DM particles could annihilate into SM particles such as γ—rays, electrons/positrons, protons/antiprotons. The total number of dark-matter particles does not change significantly after freeze-out in the early universe, but their spatial distribution changes considerably during structure formation. The DM annihilation rate could be enhanced in the center of DM halo, for example, the Galaxy center. But, nowadays there still exist many challenges in such a detection scheme. The challenges mainly come from the complication of various astrophysical processes and the limited knowledge of the cosmic rays. Even today, the origin of cosmic rays is still only partially understood, although cosmic rays were discovered almost a century ago. A possible origin of Galaxy cosmic rays (GCRs) are the superbubbles formed by OB associations [51–55]. Such a speculate is supported by many experimental observations of isotopic ratio, for example, ^{22}Ne/^{20}Ne from Ulysses [56] and CRIS [52,57]. However, superbubbles cannot be the entire solution to the origin of GCRs. For instance, superbubbles can neither account for the low large-scale anisotropy of CRs which has been found in the Milagro, ARGO, and HAWC sky [58], nor explain the shallow CR gradient deduced from γ—ray data [59]. On the other hand, the standard cosmic ray model (for example the GALPROP) lacks many physical details which are important for the CRs acceleration process before CRs are injected into the interstellar medium (ISM). For instance, the evolution of SNR, as pointed out by Blasi *et al.* [45] that the production of secondaries become significant for old SNRs ($\sim 10^4$–10^5 yr old). And as shown in Ref. [59] that the direct spectral signatures of GCR acceleration may have recently been seen in many older SNRs, such as IC 443, W28, G353.6-0.7 and perhaps W41. Both the MAGIC and VERITAS telescopes have observed TeV γ—ray emission in the direction of IC 443. This may be the signature of locally accelerated ions interacting with an ambient molecular cloud. The spectrum of IC 443 measured by the EGRET instrument on board NASA's Compton Gamma Ray Observatory also appears to show a "pion-hump" feature at about 70 MeV possibly indicating ion acceleration and interaction there.

The latest results given by AMS-02 extend up to $\sim$500 GeV in positron energy and show that the positron

fraction starts raising from ~10 GeV and remains approximately constant at energies ~200 GeV. If the positron excess is indeed due to the DM annihilations/decays, the DM mass around ~1–2 TeV would be most likely, and the annihilation cross-section/lifetime should be around $\sim(1\times10^{-24}$–$1\times10^{-23})$ cm^3 s^{-1}/ $\sim(2\times10^{26}$–$1\times10^{27})$ s (depending on the annihilation/decay channel). The implied extragalactic photon emissions from electrons and positrons severely challenge both scenarios [60]. Recently we use the measurements of the AMS-02 electron flux to derive limits on the dark matter annihilation cross section and lifetime for the specific final states of $\mu^+\mu^-$ and $\tau^+\tau^-$ and find that the dark matter annihilation (or decay) origin of the AMS-02 positron anomaly is found to be disfavored [42]. Such DM parameter rooms have also been excluded by the limitations from the gamma ray observation on the dwarf spheroidal satellite galaxies in Fermi-LAT [48]. Thus, the excess in positron fraction should contribute from the astrophysical sources. Recently, the AMS-02 antiproton-to-proton ratio data has been announced at a dedicated conference [43] and the high energy part seems to be in excess of the regular prediction of standard CR model. As a good exercise to go beyond the standard CR model, Blasi *et al.* [44,45] pointed out that positrons and antiprotons are also produced and accelerated in old SNR source. Such a scenario can explain the AMS-02 positron fraction and antiproton ratio simultaneously without any new class of source such as DM or pulsars.

The general approach to identify the energetic CR accelerators is to look for the associated high-energy gamma rays produced at the sources, since CRs are mostly charged particles and their trajectories from their sources to the Earth are deviated by the Galactic field. However, since CR electrons and nuclei can both generate gamma rays at the acceleration sites, it has not yet been possible to unambiguously associate the detected gamma radiation with sources of CR nuclei specifically. We also notice that there is no reason to require that electron and nucleic cosmic rays come from the same source. On the other hand, CRs accelerated by astrophysical sources are also expected to produce high-energy neutrinos in interactions with the ambient matter, and neutrinos interact with matter very weakly, so that they travel essentially unattenuated, and hence are excellent tracers of the sources of cosmic rays. The IceCube, Pierre Auger and Telescope Array Collaborations recently proposed that one could track the CRs sources through searching for a possible association between the high-energy neutrinos (up to at least ~2 PeV) detected by IceCube and the ultrahigh-energy cosmic rays (UHECRs) [58,61]. However, there also may exist many problems with such a method. One of them maybe that the same as the radiative signatures, the neutrinos from SNRs in the hot and low-density (5×10^{-3} cm^{-3}) medium of a superbubble interior is expected to be minimal, if the CRs come from the superbubbles (as many isotopes observations indicated). This is the so-called "missing-SNR" problem.

B. Relic density constrains from Planck data

At the early Universe, as long as the temperature T exceeds the DM mass m_χ, the DM particles were in chemical equilibrium with the other SM particles via various annihilation-production reaction:

$$\chi\bar{\chi}\rightleftharpoons\mu^+\mu^-,\qquad \tau^+\tau^-,\qquad b\bar{b},\qquad u\bar{u},\qquad W^+W^-\ldots.$$

The temperature T and DM density drop as a result of the overall adiabatic expansion of the Universe, the DM population becomes nonrelativistic and the annihilations take over the thermal productions. The reaction will stop when the DM density is so low that they fail to annihilate with each other. At around the temperature that the reaction rate fell below the expansion rate H, the DM particles began to decouple from the thermal bath. The resulting freeze-out occurs typically for values of the mass-to-temperature $x_{\rm F}=m_\chi/T_{\rm F}\sim20$. Then, the DM number density n_χ remains subsequently constant per-covolume (volume that expands with the expanding universe) and becomes the relic density that we observe today [1,25,62]. The evolution of DM number density n_χ is described by the Boltzmann equation,

$$\frac{dn_\chi}{dt}=-3Hn_\chi-\langle\sigma_{\rm ann}v\rangle(n_\chi^2-(n_\chi^{\rm eq})^2), \tag{1}$$

where $n_\chi^{\rm eq}$ is the number density at thermal equilibrium

$$n_\chi^{\rm eq}=g\left(\frac{m_\chi^2}{2\pi x}\right)^{3/2}{\rm e}^{-x}, \tag{2}$$

where $x=m_\chi/T$, $\langle\sigma_{\rm ann}v\rangle$ is the total annihilation cross-section multiplied by velocity, brackets denote thermal average, it can be approximated with the nonrelativistic expansion in powers of v^2

$$\langle\sigma_{\rm ann}v\rangle\simeq a+6b/x. \tag{3}$$

Then the relic density of DM is found to be

$$\Omega_\chi h^2\simeq\frac{1.07\times10^9\ {\rm GeV}^{-1}}{M_{\rm pl}}\frac{x_{\rm F}}{\sqrt{g_*}}\frac{1}{(a+3b/x_{\rm F})} \tag{4}$$

$$\simeq\frac{3\times10^{-27}\ {\rm cm}^3\ {\rm s}^{-1}}{\langle\sigma_{\rm ann}v\rangle} \tag{5}$$

where $h=H_0/100$ kms^{-1} Mpc^{-1} is the Hubble parameter, $M_{\rm pl}$ is Planck mass, $g_*\sim100$ is evaluated at the freeze-out temperature.

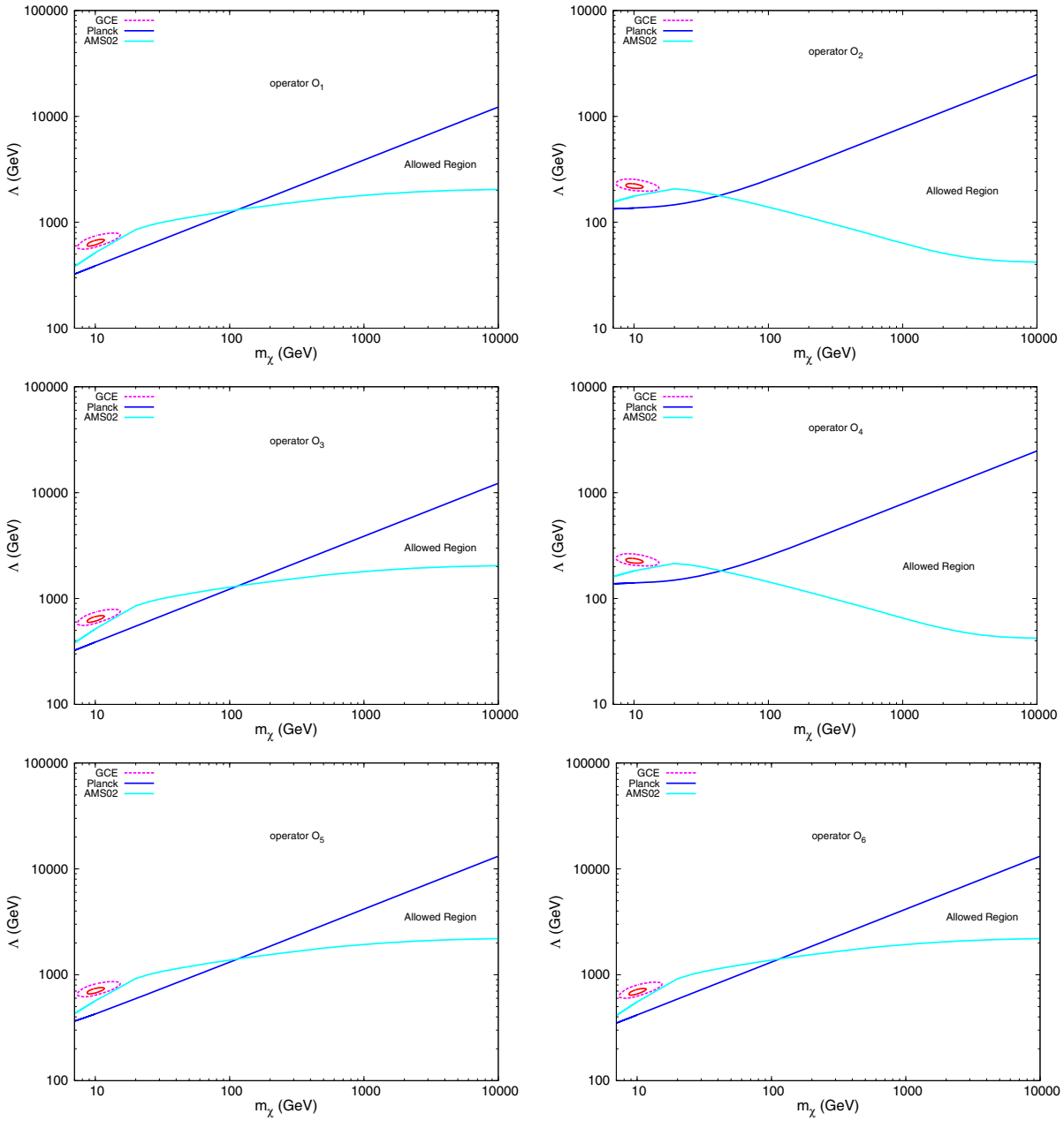

FIG. 2. Bounds on effective theory parameters and favored regions to explain the GCE as a function of DM mass m_χ. The blue lines are the constraints from Planck DM relic density observes, and the light blue lines are the AMS-02 experiment bounds. The cycle regions corresponding to good fits to the GCE at 3σ C.L. Lower the blue line and upper the light blue line is the allowed region.

The results from CMB experiments shown that the evolutions of the Universe are remarkably consistent with the predictions of the ΛCDM cosmological model. This model is based upon a spatially-flat, expanding Universe whose dynamics are governed by general relativity and whose constituents are dominated by cold dark matter (CDM) and a cosmological constant (Λ) at late times [63]. In such a scenario, the CDM relic density from recently Planck result is $\Lambda_{\rm CDM}h^2 = 0.1199 \pm 0.0027$ [63]. The annihilation cross-section of DM particle should be $\langle\sigma_{\rm ann}v\rangle \sim 3\times10^{-26}$ cm^3 s^{-1} with the assumption that the measured $\Lambda_{\rm CDM}h^2$ contributes from a single DM component. This is exactly the size of the cross section that one expects from a weak interaction process. However, in general, the species of DM particles should be more than one, thus we should require that the resulting of relic density of each operator to be less than the measured value from CMB experiment. In other words, the relic density from Planck experiment puts an upper limit on the heavy mass scale Λ for each operator.

The calculation results of the annihilation cross section for each operator are shown in the Appendix. And the limits

on the mass scale Λ from Planck experiment are shown in Figs. 2–4. Combining with the constrains from AMS-02, we find that most of the interaction operators have been excluded, the operators remaining available are $\mathcal{O}_7$, $\mathcal{O}_9$ and $\mathcal{O}_{12}$.

C. Interactions at loop-level and direct detection

The direct detection involves the construction of deep underground particle detectors to directly register the interactions of through-going dark matter particles. The WIMP-nucleon total interaction rate is highly model-dependent and subject to many orders of magnitude uncertainty. In the nonrelativistic (NR) limit, WIMP-nucleon couplings can be classified into "spin-independent" (SI) and "spin-dependent" (SD). For the former case, the spin orientations do not affect the amplitude. If all nucleons couple to WIMPs in the same way, the total nuclear cross-section is enhanced by the square of the atomic mass due to coherent summation over all the scattering centers in the nucleus. This greatly increases event rates on heavy target nuclei relative to lighter nuclei. For the latter case, the sign of the scattering amplitude depends on the relative orientation of particle spins. The WIMP effectively couples to the net nuclear spin, due to cancellation between opposite spin pairs. It will differ depending on whether the net nuclear spin is carried primarily by a residual neutron or proton [64].

Above we have assumed that WIMPs only interact with τ lepton at tree-level, thus such a DM particle neither interacts with electrons nor with nucleons at tree-level in a detector. However, there are model independent couplings to quarks induced at loop-level from photon exchange between virtual leptons and the quarks [24]. Such interaction diagrams at loop-level are shown in Fig. 5. The shaded loop represents dark gauge interaction between WIMPs and τ leptons. The virtual τ leptons running in the loop are induced by the vacuum fluctuations; it conducts the interaction between DM and quarks through the photon exchange. Here we only consider four types of interaction: $\mathcal{O}_1$, $\mathcal{O}_5$, $\mathcal{O}_7$, $\mathcal{O}_{13}$. Other types of interaction are not taken into account in this subsection for the following reasons: (i) most of the effective interactions have been excluded by the relic density constrains from Planck experiment, (ii) the above operators have non-null interactions with quarks induced at loop-level, while for pseudoscalar and axial-vector lepton currents, the diagrams vanish to all loop orders [24], (iii) the effective interactions are strongly suppressed (N/A) (see Table I). The scattering cross section of WIMPs and nucleons are read as follows [24]

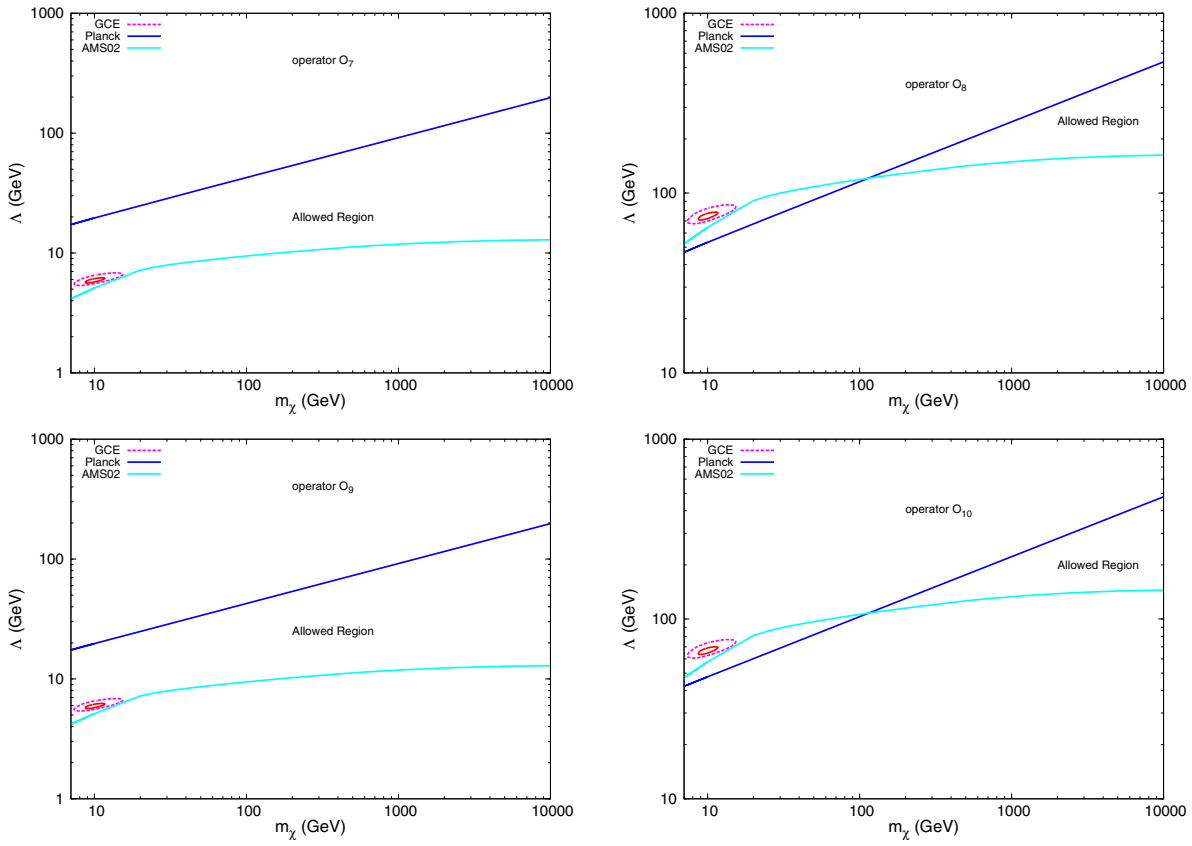

FIG. 3. Bounds on effective theory parameters and favored regions to explain the GCE as a function of DM mass m_χ. The blue lines are the constrains from Planck DM relic density observes, and the light blue lines are the AMS-02 experiment bounds. The cycle regions corresponding to good fits to the GCE at 3σ C.L. Lower the blue line and upper the light blue line is the allowed region.

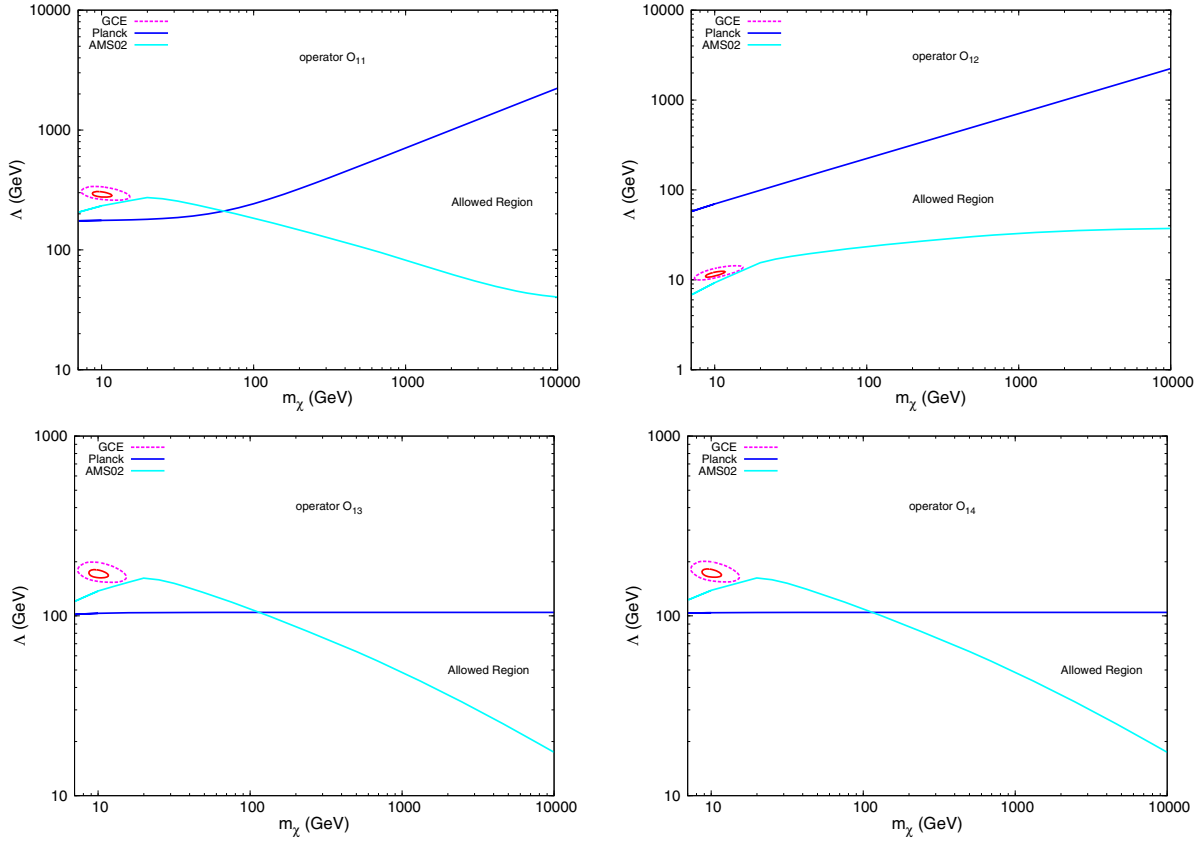

FIG. 4. Bounds on effective theory parameters and favored regions to explain the GCE as a function of DM mass m_χ. The blue lines are the constrains from Planck DM relic density observes, and the light blue lines are the AMS-02 experiment bounds. The cycle regions corresponding to good fits to the GCE at 3σ C.L. The lower blue line and the upper light blue line is the allowed region.

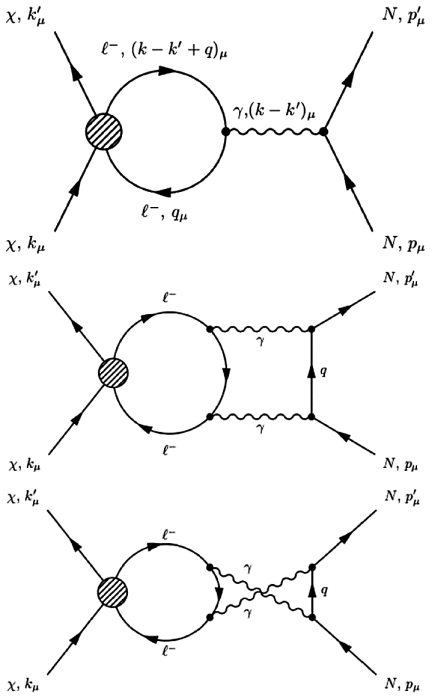

FIG. 5. DM-nucleons interactions induced at loop-level.

$$\sigma_1 = \sigma_1^0 \frac{1}{9}\left[\log\left(\frac{m_f^2}{\Lambda_1^2}\right)\right]^2 \tag{6}$$

$$\sigma_5 = \sigma_5^0\left[\log\left(\frac{m_f^2}{\Lambda_5^2}\right)\right]^2 \frac{m_f^2}{\mu_N^2}\log\left(\frac{E_d^{\max}}{E_d^{\min}}\right) \tag{7}$$

$$\sigma_7 = 2\sigma_7^0\left(\frac{\pi\alpha Z}{12}\right)^2\left(\frac{\mu_N v}{\Lambda_7}\right)^2 \tag{8}$$

$$\sigma_{13} = 2\sigma_{13}^0\left(\frac{\pi\alpha Z}{12}\right)^2\left(\frac{\mu_N v}{2m_\chi}\right)^2, \tag{9}$$

where

$$\sigma_i^0 \simeq 1.9\times 10^{-32}\ \mathrm{cm}^2\left(\frac{\Lambda_i}{10\ \mathrm{GeV}}\right)^{-4}\left(\frac{\mu_N}{10\ \mathrm{GeV}}\right)^2\left(\frac{Z}{53}\right)^2, \tag{10}$$

where $i = 1, 5, 7, 13$ stands for the coefficients of scattering cross section described in Eq. (6)–Eq. (9), $\mu_N = m_N m_\chi/(m_N + m_\chi)$ is the reduced mass of the two-particle system, α is the fine structure constant, m_N is the nucleus mass, m_f is the mass of τ lepton, Z is the charge of nucleus, $v \sim 10^{-3}$ is

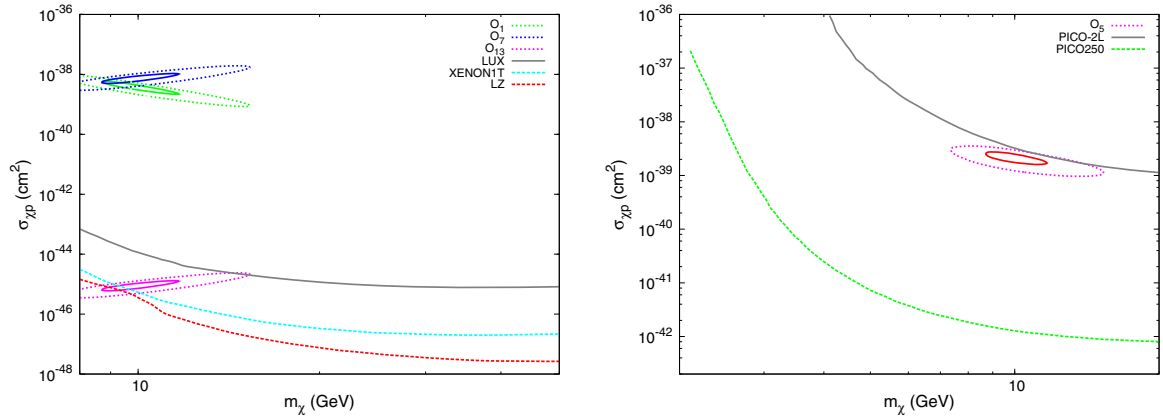

FIG. 6. Left panel: spin-independent DM-nucleons scattering cross section as a function of DM mass m_χ, the solid (dot) cycle corresponding to 1σ (3σ) contours, and the solid grey line is the upper limits of DM-nucleon scattering cross section at 90% C.L. from LUX measurements [65]. Right panel: spin-dependent DM-nucleon scattering cross section as a function of DM mass m_χ, the solid (dot) cycle corresponding to 1σ (3σ) contours, and the solid grey line is the upper limits of DM-nucleon scattering cross section at 90% C.L. from PICO measurements [66]. The dashed lines are the upper limits of DM-nucleon scattering cross section at 90% C.L. from Ref. [64].

WIMPs relative velocity in unit light speed c, and $E_d \sim$ keV is the recoil energy of the nucleus in $\chi - N$ scattering.

We demonstrate the results in Fig. 6, the cross sections at 3σ C.L. are derived from the DM fit results of Fermi GeV excess [18]. In the left panel of Fig. 6 we show the results of spin-independent $\chi - N$ scattering cross section. We find that the cross sections of operator $\mathcal{O}_1$ and $\mathcal{O}_7$ are much larger than the 90% up-limit given by the LUX experiment, thus have been excluded as suitable DM-lepton interactions for the Galactic Center excess. The cross section of operator $\mathcal{O}_1 \propto \Lambda_1^{-4}$, and it is not suppressed by WIMPs relative velocity v^2. For the cross section of operator $\mathcal{O}_7$, it is suppressed both by a factor Λ_7^{-6} and the WIMPs relative velocity v^2, however, the mass scale of this operator is $\Lambda_7 \sim 6$ GeV, which is much lower than other operators. The operator $\mathcal{O}_{13}$ is still allowed by the LUX experiment. We can see that its scattering cross section is much less than other type of operators, because the mass scale $\Lambda_{13} \sim$ (160–200) GeV, the cross section is proportional to Λ_{13}^{-4} and the cross section σ_{13} is also suppressed by WIMPs relative velocity v^2. But we notice that the 3σ results is not far below the LUX up-limit so it may be excluded by the near future experiment. In the right panel of Fig. 6 we demonstrate the result of spin-dependent $\chi - N$ scattering cross section, and find out that the cross section of $\mathcal{O}_5$ at 3σ C.L. is still allowed by the PICO experiment. Since the corresponding mass scale of operator $\mathcal{O}_5$ is $\Lambda_5 \sim$ (600–800) GeV, and the cross section is suppressed by a factor Λ_5^{-4} and the fermion mass m_f. In the Fig. 6 we also show the possible constraints from the next generation (G3) experimental (XENON1T and LZ) and US-led direct detection experiments that are expected to operate over the next decade (PICO250) [64]. We can see that all of the effective interactions will be excluded if null signals are found in future direct detection experiments.

In this section, we have taken into account the constraints on the effective interactions from DM relic density observation, direct and indirect detection, we find that most of the interactions have been excluded, the available operators remaining are $\mathcal{O}_9$ and $\mathcal{O}_{12}$.

V. SUMMARY AND DISCUSSION

In this work, with consideration of the limits on the dark matter annihilation cross-section which we obtained in our recent work [30] and the 3σ fit results of DM parameter space using the Fermi-LAT data [18], we find that most of DM annihilation channels have been excluded except for the τ lepton channel. Thus we assume that the dark matter only couples with τ lepton directly but does not interact with other standard model particles at tree-level. We describe the interactions with a general effective field theory approach by using higher-dimensional operators, and this approach provides for a model independent analysis. Then we consider the constraints from the measurement of the DM relic density in the Planck experiment and the AMS-02 cosmic rays experiment and find that most of the interaction operators except $\mathcal{O}_7$, $\mathcal{O}_9$ and $\mathcal{O}_{12}$ have been excluded. However, even in such a scenario there are loop induced dark matter-nucleon interactions. We calculate the DM-nucleon scattering cross section induced at loop-level and take into account the limits on the scattering cross section from direct detection experiments LUX and PICO, and we find that the scalar-type interaction $\mathcal{O}_1$ and vector-type interaction $\mathcal{O}_7$ have been excluded, while the tensor-type interaction $\mathcal{O}_5$ and complex scalar DM-lepton interaction $\mathcal{O}_{13}$ are still allowed. We further consider the possible constrains from the next generation (G3) experimental (XENON1T and LZ) and US-led direct detection experiments that are expected to operate over the next decade (PICO250) [64], and we find that the interactions $\mathcal{O}_5$ and $\mathcal{O}_{13}$ will also be excluded in near-future

direct detections. Thus, the operators we consider that remain available for explaining the GCE are $\mathcal{O}_9$ and $\mathcal{O}_{12}$.

In this work, one of the main constraints comes from the AMS-02 experiment, and as shown in Ref. [30], the solar modulation plays an important role in modifying the constraints on the dark matter annihilation cross section and lifetime for DM mass $m_\chi < 100$ GeV, and thus the solar modulation is also crucial for the DM interpretation of the GCE. The strength of the solar modulation depends on the solar activity which can be represented by a tilt angle α ($30° \lesssim \alpha \lesssim 70°$, it describes the region swept by the heliospheric current sheet) and the polarity of solar magnetic field A_c. The larger the tilt angle α is the stronger the solar modulation is, and the solar modulation is much stronger in cycle $qA_c < 0$ than in cycle $qA_c > 0$ (where q is the charge of CRs). Constraints on DM parameters from AMS-02 positron fraction data would become more stringent when the solar modulation is weak. Thus constraints on DM parameters from AMS-02 positron fraction data will be most stringent for the DM mass $m_\chi < 100$ GeV at the year of $\sim$2018 when the tilt angle $\alpha \sim 30°$ and $qA_c > 0$ for the positron. We may expect that the τ channel will also be excluded by AMS-02 positron fraction data at that time and the DM interpretation of the GCE will no longer be suitable.

ACKNOWLEDGMENTS

This work is supported in part by the National Natural Science Foundation of China (under Grants No. 11275097, No. 11475085 and No. 11535005).

APPENDIX: ANNIHILATION CROSS SECTION FORMULAS

Here we show the calculation results of the annihilation cross section of the operators shown in Table I, v is WIMPs' relative velocity in unit c, $\Lambda = \frac{M}{g_\chi g_f}$, M is the mass of the exchanged particle, g_χ and g_f are the couplings.

$$\langle\sigma_1 v\rangle = \frac{1}{48\pi\Lambda_1^4}\sqrt{1-\frac{m_f^2}{m_\chi^2}}\left(24(2m_\chi^2+m_f^2) + \frac{8m_\chi^4-4m_\chi^2m_f^2+5m_f^4}{m_\chi^2-m_f^2}\langle v^2\rangle\right) \tag{A1}$$

$$\langle\sigma_2 v\rangle = \frac{1}{48\pi\Lambda_2^4}\sqrt{1-\frac{m_f^2}{m_\chi^2}}\left(21m_f^2 + \frac{8m_\chi^4-4m_\chi^2m_f^2+5m_f^4}{m_\chi^2-m_f^2}\langle v^2\rangle\right) \tag{A2}$$

$$\langle\sigma_3 v\rangle = \frac{1}{48\pi\Lambda_3^4}\sqrt{1-\frac{m_f^2}{m_\chi^2}}\left(48m_\chi^2-27m_f^2 + \frac{8m_\chi^4-4m_\chi^2m_f^2+5m_f^4}{m_\chi^2-m_f^2}\langle v^2\rangle\right) \tag{A3}$$

$$\langle\sigma_4 v\rangle = \frac{1}{48\pi\Lambda_4^4}\sqrt{1-\frac{m_f^2}{m_\chi^2}}\left(24m_f^2 + \frac{8m_\chi^4-22m_\chi^2m_f^2+17m_f^4}{m_\chi^2-m_f^2}\langle v^2\rangle\right) \tag{A4}$$

$$\langle\sigma_5 v\rangle = \frac{1}{6\pi\Lambda_5^4}\sqrt{1-\frac{m_f^2}{m_\chi^2}}\left(12m_\chi^2+45m_f^2 + \frac{2m_\chi^4+2m_\chi^2m_f^2+5m_f^4}{m_\chi^2-m_f^2}\langle v^2\rangle\right) \tag{A5}$$

$$\langle\sigma_6 v\rangle = \frac{1}{6\pi\Lambda_6^4}\sqrt{1-\frac{m_f^2}{m_\chi^2}}\left(12m_\chi^2+9m_f^2 + \frac{2m_\chi^4+2m_\chi^2m_f^2+5m_f^4}{m_\chi^2-m_f^2}\langle v^2\rangle\right) \tag{A6}$$

$$\langle\sigma_7 v\rangle = \frac{m_f^2}{8\pi\Lambda_7^6}\sqrt{1-\frac{m_f^2}{m_\chi^2}}(m_\chi^2-m_f^2)\langle v^2\rangle \tag{A7}$$

$$\langle\sigma_8 v\rangle = \frac{m_f^2}{2\pi\Lambda_8^6}\sqrt{1-\frac{m_f^2}{m_\chi^2}}(m_\chi^2-m_f^2) \tag{A8}$$

$$\langle\sigma_9 v\rangle = \frac{m_f^2}{8\pi\Lambda_9^6}\sqrt{1-\frac{m_f^2}{m_\chi^2}}m_\chi^2\langle v^2\rangle \tag{A9}$$

$$\langle\sigma_{10} v\rangle = \frac{m_f^2}{16\pi\Lambda_{10}^6}\sqrt{1-\frac{m_f^2}{m_\chi^2}}m_\chi^2\left(8+\frac{2m_\chi^2-m_f^2}{m_\chi^2-m_f^2}\langle v^2\rangle\right) \tag{A10}$$

$$\langle\sigma_{11} v\rangle = \frac{1}{24\pi\Lambda_{11}^4}\sqrt{1-\frac{m_f^2}{m_\chi^2}}\left(48m_f^2 + \frac{4m_\chi^4-8m_\chi^2m_f^2-5m_f^4}{m_\chi^2-m_f^2}\langle v^2\rangle\right) \tag{A11}$$

$$\langle\sigma_{12} v\rangle = \frac{1}{24\pi\Lambda_{12}^4}\sqrt{1-\frac{m_f^2}{m_\chi^2}}\left(\frac{4m_\chi^4-8m_\chi^2m_f^2-5m_f^4}{m_\chi^2-m_f^2}\langle v^2\rangle\right) \tag{A12}$$

$$\langle\sigma_{13} v\rangle = \frac{m_f^2}{4\pi\Lambda_{13}^4}\sqrt{1-\frac{m_f^2}{m_\chi^2}}\left(1-\frac{m_f^2}{m_\chi^2}\right) \tag{A13}$$

$$\langle\sigma_{14} v\rangle = \frac{m_f^2}{4\pi\Lambda_{14}^4}\sqrt{1-\frac{m_f^2}{m_\chi^2}} \tag{A14}$$

[1] G. Bertonea and D. Hooper, Phys. Rep. **405**, 279 (2005).
[2] K. A. Olive, arXiv:astro-ph/0301505.
[3] K. Griest and M. Kamionkowski, Phys. Rep. **333–334**, 167 (2000).
[4] R. Essig *et al.*, arXiv:1311.0029v1.
[5] L. Goodenough and D. Hooper, arXiv:0910.2998.
[6] The Fermi-LAT Collaboration, arXiv:0912.3828.
[7] D. Hooper and L. Goodenough, Phys. Lett. B **697**, 412 (2011).
[8] T. Daylan, D. P. Finkbeiner, D. Hooper, T. Linden, S. K. N. Portillo, N. L. Rodd, and T. R. Slatyer, Phys. Dark Univ. **12**, 1 (2016).
[9] B. Zhou, Y. F. Liang, X. Y. Huang, X. Li, Y. Z. Fan, L. Feng, and J. Chang, Phys. Rev. D **91**, 123010 (2015).
[10] The Fermi-LAT Collaboration, arXiv:1511.02938.
[11] The Fermi-LAT Collaboration, Astrophys. J. **750**, 3 (2012).
[12] A. Berlin and D. Hooper, Phys. Rev. D **89**, 016014 (2014).
[13] D. Hooper, I. Cholis, T. Linden, J. M. Siegal-Gaskins, and T. R. Slatyer, Phys. Rev. D **88**, 083009 (2013).
[14] F. Calore, M. Di Mauro, and F. Donato, Astrophys. J. **796**, 14 (2014).
[15] O. Macias and C. Gordon, Phys. Rev. D **89**, 063515 (2014).
[16] K. N. Abazajian, N. Canac, S. Horiuchi, and M. Kaplinghat, Phys. Rev. D **90**, 023526 (2014).
[17] F. Calore, I. Cholis, and C. Weniger, J. Cosmol. Astropart. Phys. 03 (2015) 038C.
[18] F. Calore, I. Cholis, C. McCabe, and C. Weniger, Phys. Rev. D **91**, 063003 (2015).
[19] D. Hooper and T. Linden, Phys. Rev. D **84**, 123005 (2011).
[20] C. Gordon and O. Macias, Phys. Rev. D **88**, 083521 (2013).
[21] M. Cirelli, D. Gaggero, G. Giesen, M. Taoso, and A. Urbano, J. Cosmol. Astropart. Phys. 12 (2014) 045C.
[22] J. Goodman, M. Ibe, A. Rajaraman, W. Shepherd, Tim M. P. Tait, and H. B. Yu, Phys. Rev. D **82**, 116010 (2010).
[23] Y. Bai, P. J. Fox, and R. Harnik, J. High Energy Phys. 12 (2010) 048.
[24] J. Kopp, V. Niro, T. Schwetz, and J. Zupan, Phys. Rev. D **80**, 083502 (2009).
[25] K. Cheung, P. Y. Tseng, Y. L. S. Tsai, and T. C. Yuan, J. Cosmol. Astropart. Phys. 05 (2012) 001.
[26] P. J. Fox, R. Harnik, J. Kopp, and Y. Tsai, Phys. Rev. D **84**, 014028 (2011).
[27] F. D'Eramo and M. Procura, J. High Energy Phys. 04 (2015) 054.
[28] K. P. Modak, arXiv:1509.00874.
[29] A. Alves, S. Profumo, F. S. Queiroz, and W. Shepherd, Phys. Rev. D **90**, 115003 (2014).
[30] B. Q. Lu and H. S. Zong, arXiv:1510.04032.
[31] S. Profumo and W. Shepherd, Phys. Rev. D **88**, 056018 (2013).
[32] D. Alves *et al.*, J. Phys. G **39**, 105005 (2012).
[33] J. Alwall, P. Schuster, and N. Toro, Phys. Rev. D **79**, 075020 (2009).
[34] R. Essig, E. Izaguirre, J. Kaplan, and J. G. Wacker, J. High Energy Phys. 01 (2012) 074.
[35] A. DiFranzo, K. I. Nagao, A. Rajaraman, and T. M. P. Tait, J. High Energy Phys. 11 (2013) 014.
[36] O. Buchmueller, M. J. Dolan, and C. McCabe, J. High Energy Phys. 01 (2014) 025.
[37] M. T. Frandsen, F. Kahlhoefer, S. Sarkar, and K. Schmidt-Hoberg, J. High Energy Phys. 09 (2011) 128.
[38] M. T. Frandsen, F. Kahlhoefer, A. Preston, S. Sarkar, and K. Schmidt-Hoberg, J. High Energy Phys. 07 (2012) 123.
[39] M. Aguilar *et al.* (AMS Collaboration), Phys. Rev. Lett. **110**, 141102 (2013).
[40] L. Bergström, T. Bringmann, I. Cholis, D. Hooper, and C. Weniger, Phys. Rev. Lett. **111**, 171101 (2013).
[41] A. Ibarra, A. S. Lamperstorfer, and J. Silk, Phys. Rev. D **89**, 063539 (2014).
[42] B. Q. Lu and H. S. Zong, Phys. Rev. D **92**, 103002 (2015).
[43] AMS-02 Collaboration, "AMS Days at CERN" and Latest Results, 15, April, 2015 (to be published).
[44] P. Blasi, Phys. Rev. Lett. **103**, 051104 (2009).
[45] P. Blasi and P. D. Serpico, Phys. Rev. Lett. **103**, 081103 (2009).
[46] P. Mertsch and S. Sarkar, Phys. Rev. Lett. **103**, 081104 (2009).
[47] P. Mertsch and S. Sarkar, Phys. Rev. D **90**, 061301 (2014).
[48] M. Ackermann *et al.* (The Fermi LAT Collaboration), Phys. Rev. Lett. **115**, 231301 (2015).
[49] T. Lacroix, C. Boehm, and J. Silk, Phys. Rev. D **90**, 043508 (2014).
[50] A. Dedes, I. Giomataris, K. Suxho, and J. D. Vergados, Nucl. Phys. B **826**, 148 (2010).
[51] M. Cassé and J. A. Paul, Astrophys. J. **258**, 860 (1982).
[52] W. R. Binns *et al.*, Astrophys. J. **634**, 351 (2005).
[53] W. R. Binns *et al.*, New Astron. Rev. **52**, 427 (2008).
[54] J. C. Higdon and R. E. Lingenfelter, Astrophys. J. **590**, 822 (2003).
[55] J. C. Higdon and R. E. Lingenfelter, Adv. Space Res. **37**, 1913 (2006).
[56] J. J. Connell and J. A. Simpson, in *Proc. 25th Int. Cosmic Ray Conf. (Durban)* (Int. Cosmic Ray Conf., Durban, 1997) vol. 3, p. 381.
[57] W. R. Binns , in AIP Conf. Proc. **598**, 257 (2001).
[58] D. Fargion, P. Oliva, and G. Ucci, *Proc. Sci.*, FRAPWS2014 (2016) 028 [arXiv:1512.08794].
[59] Y. Butt, Nature (London) **460**, 701 (2009).
[60] M. Klasen, M. Pohl, and G. Sigl, Prog. Part. Nucl. Phys. **85**, 1 (2015).
[61] The IceCube, Pierre Auger and Telescope Array Collaborations, J. Cosmol. Astropart. Phys. 01 (2016) 037.
[62] P. Salati, Phys. Lett. B **571**, 121 (2003).
[63] P. A. R. Ade *et al.* (Planck Collaboration), Astron. Astrophys. **571**, A16 (2014).
[64] P. Cushman *et al.*, arXiv:1310.8327.
[65] D. S. Akerib *et al.* (LUX Collaboration), Phys. Rev. Lett. **112**, 091303 (2014).
[66] C. Amole *et al.* (PICO Collaboration), Phys. Rev. Lett. **114**, 231302 (2015).